

Supporting Information (SI)

LearnCK: Mass Conserving Neural Network Reduction of Chemical Reaction Mechanisms and Species

*Sashank Kasiraju¹ and Dionisios G. Vlachos^{*1,2}*

¹RAPID Manufacturing Institute and Delaware Energy Institute, 221 Academy St., University of Delaware, Newark, Delaware 19716, USA

²Department of Chemical and Biomolecular Engineering, 150 Academy St., University of Delaware, Newark, Delaware 19716, USA

Corresponding Author: *D. G. Vlachos: vlachos@udel.edu

SI-1: Microkinetic model (MKM) for ammonia reduction on Ruthenium catalyst

The list of elementary steps for this MKM are shown below. Here Ru(T) and Ru(S) are the terrace and step sites of the Ru surface. This model has 3 gas phase species, 14 surface species on two sites, and a total of 14 reactions.

1. $\text{H}_2 + 2 \text{RU(T)} \rightleftharpoons 2 \text{H(T)}$
2. $\text{N}_2 + \text{RU(T)} \rightleftharpoons \text{N}_2(\text{T})$
3. $\text{NH}_3 + \text{RU(T)} \rightleftharpoons \text{NH}_3(\text{T})$
4. $\text{N}_2 + \text{RU(S)} \rightleftharpoons \text{N}_2(\text{S})$
5. $\text{H}_2 + 2 \text{RU(S)} \rightleftharpoons 2 \text{H(S)}$
6. $\text{NH}_3 + \text{RU(S)} \rightleftharpoons \text{NH}_3(\text{S})$
7. $\text{NH}_3(\text{T}) + \text{RU(T)} \rightleftharpoons \text{H(T)} + \text{NH}_2(\text{T})$
8. $\text{NH}_2(\text{T}) + \text{RU(T)} \rightleftharpoons \text{H(T)} + \text{NH(T)}$
9. $\text{NH(T)} + \text{RU(T)} \rightleftharpoons \text{H(T)} + \text{N(T)}$
10. $\text{N}_2(\text{T}) + \text{RU(T)} \rightleftharpoons 2 \text{N(T)}$
11. $\text{NH}_3(\text{S}) + \text{RU(S)} \rightleftharpoons \text{H(S)} + \text{NH}_2(\text{S})$
12. $\text{NH}_2(\text{S}) + \text{RU(S)} \rightleftharpoons \text{H(S)} + \text{NH(S)}$
13. $\text{NH(S)} + \text{RU(S)} \rightleftharpoons \text{H(S)} + \text{N(S)}$
14. $\text{N}_2(\text{S}) + \text{RU(S)} \rightleftharpoons 2 \text{N(S)}$

Example MKM can be found at this GitHub repository:

<https://github.com/VlachosGroup/openMKM-SI-examples/tree/main/Example-2-NH3-formation-on-Ru/lateral-yes>

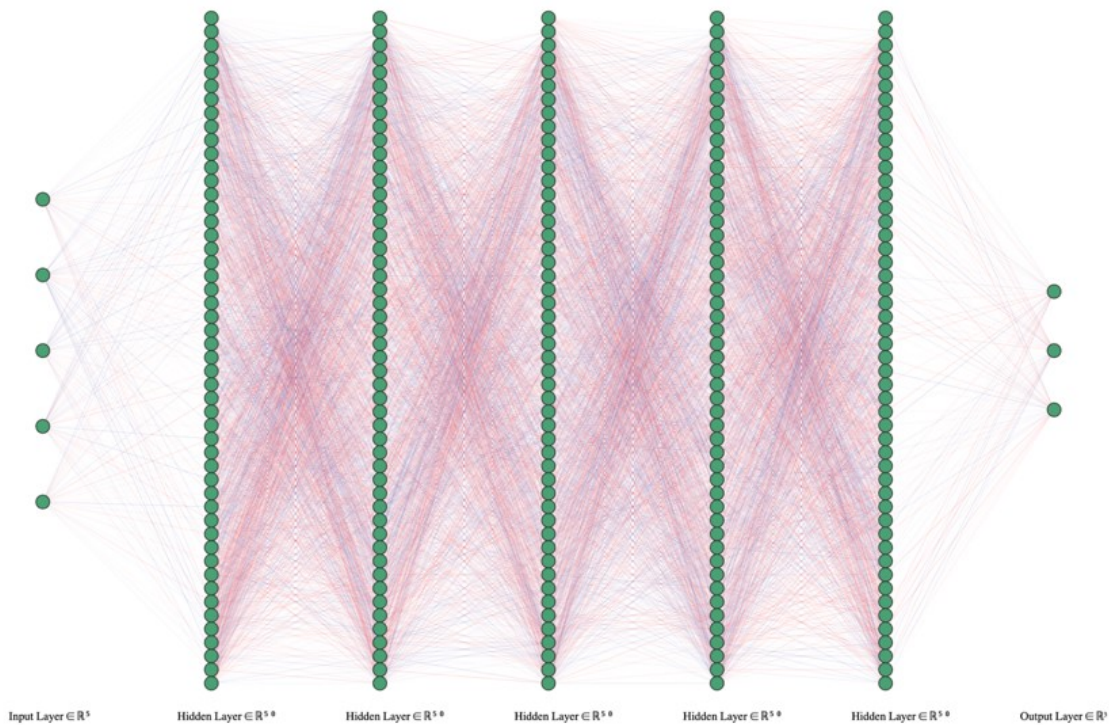


Figure S1. Pictorial representation of a typical Deep Neural Network for the ammonia reduction model. The DNN has 5 input nodes for 5 features P , T , X_{NH_3} , X_{H_2} , X_{N_2} , 5 hidden layers each with 50 neurons with the RELU activation function, and three output nodes for the turnover frequencies of three major species (NH_3 , N_2 , H_2).

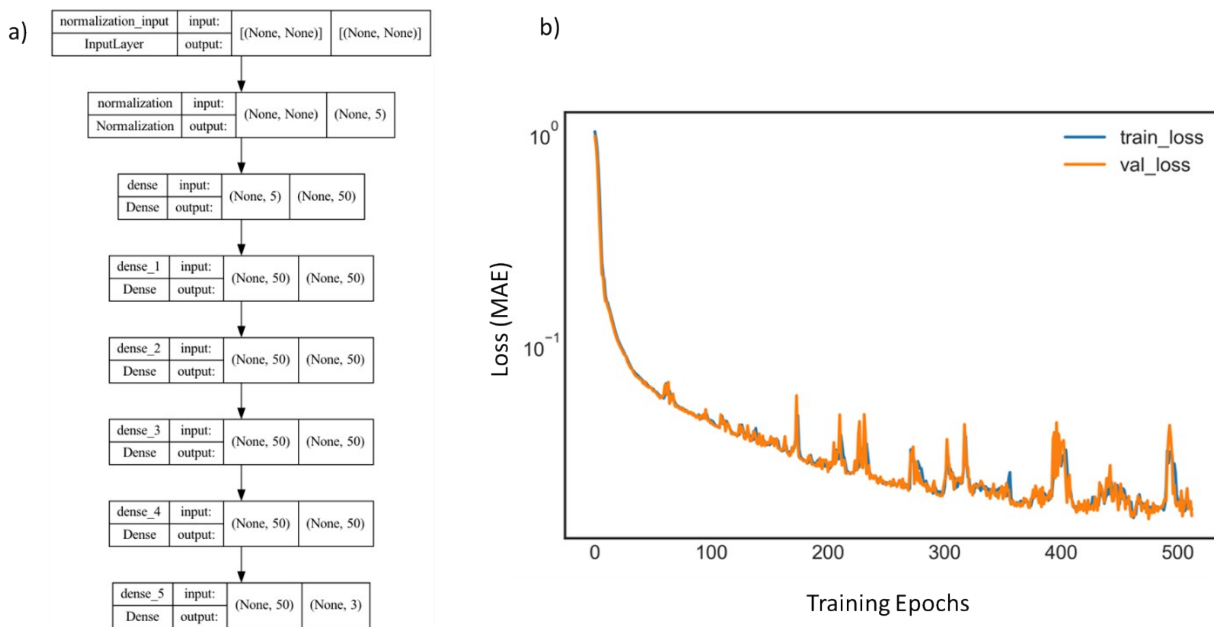


Figure S2. a) TensorFlow-Keras model summary of the 5-layer DNN shown in the Figure S1. b) Training curve: training and validation error as a function of training epochs using the Adam optimizer with a learning rate of 0.01.

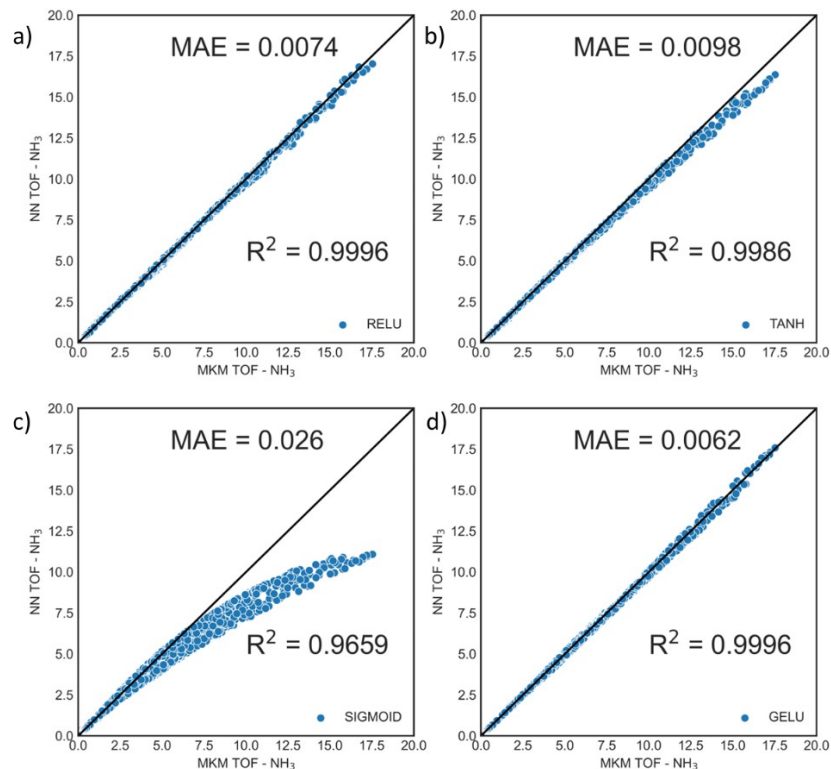


Figure S3 Parity for NH_3 TOF predictions using a DNN (y-axis) vs. the MKM (x-axis) simulation. The effect of the activation function for a 5-layer deep DNN with 50 neurons in each layer is given for the a) rectified linear unit (RELU), b) hyperbolic tangent (TANH), c) sigmoid, and d) Gaussian error linear unit (GELU) activation functions.

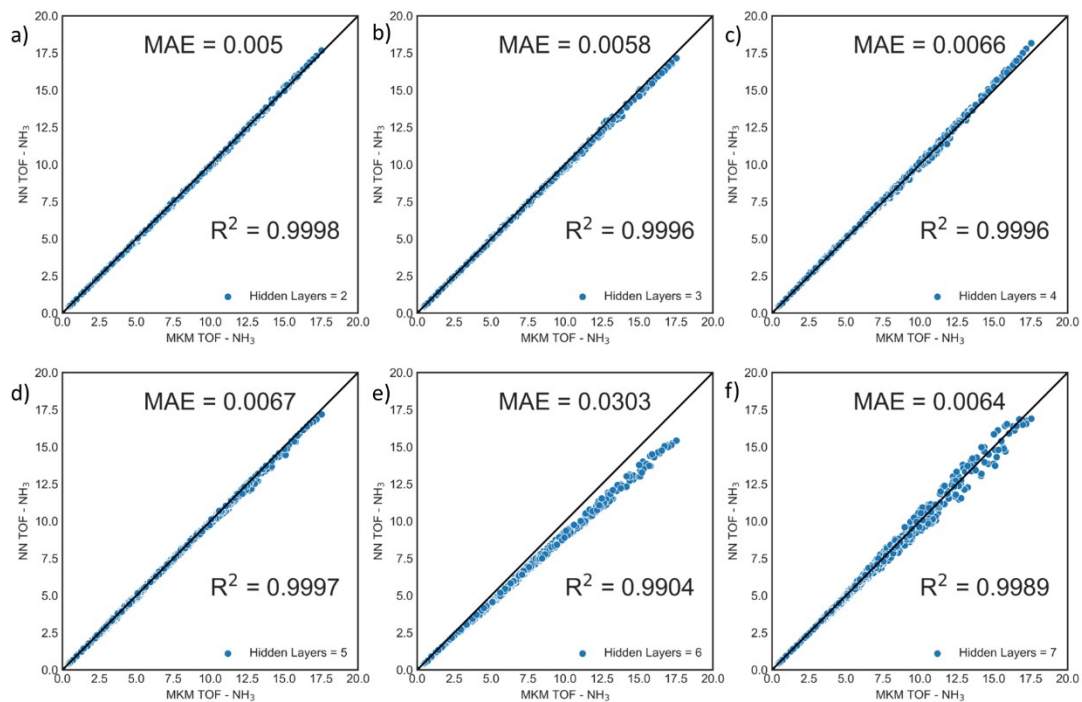


Figure S4 Parity for NH_3 TOF predictions using a DNN (y-axis) vs. the MKM (x-axis) simulation. The effect of the number of hidden layers (depth) of the DNN with 50 neurons in each layer and the GELU activation function is given for the (2 - 7 layers) from a) 2 to f) 7.

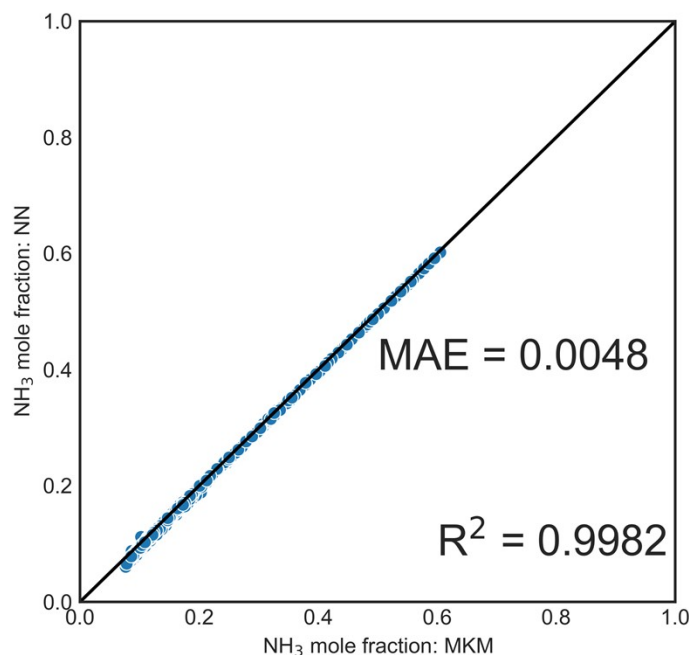


Figure S5. Parity for NH_3 mole-fraction from 1,200 PFR simulations using a DNN-surrogate Python-ODE solver model (y-axis) vs. from the MKM (x-axis) simulation. TOFs of the NH_3 are trained and predicted by the surrogate model, and the rest of the TOFs are calculated using the reaction stoichiometry.

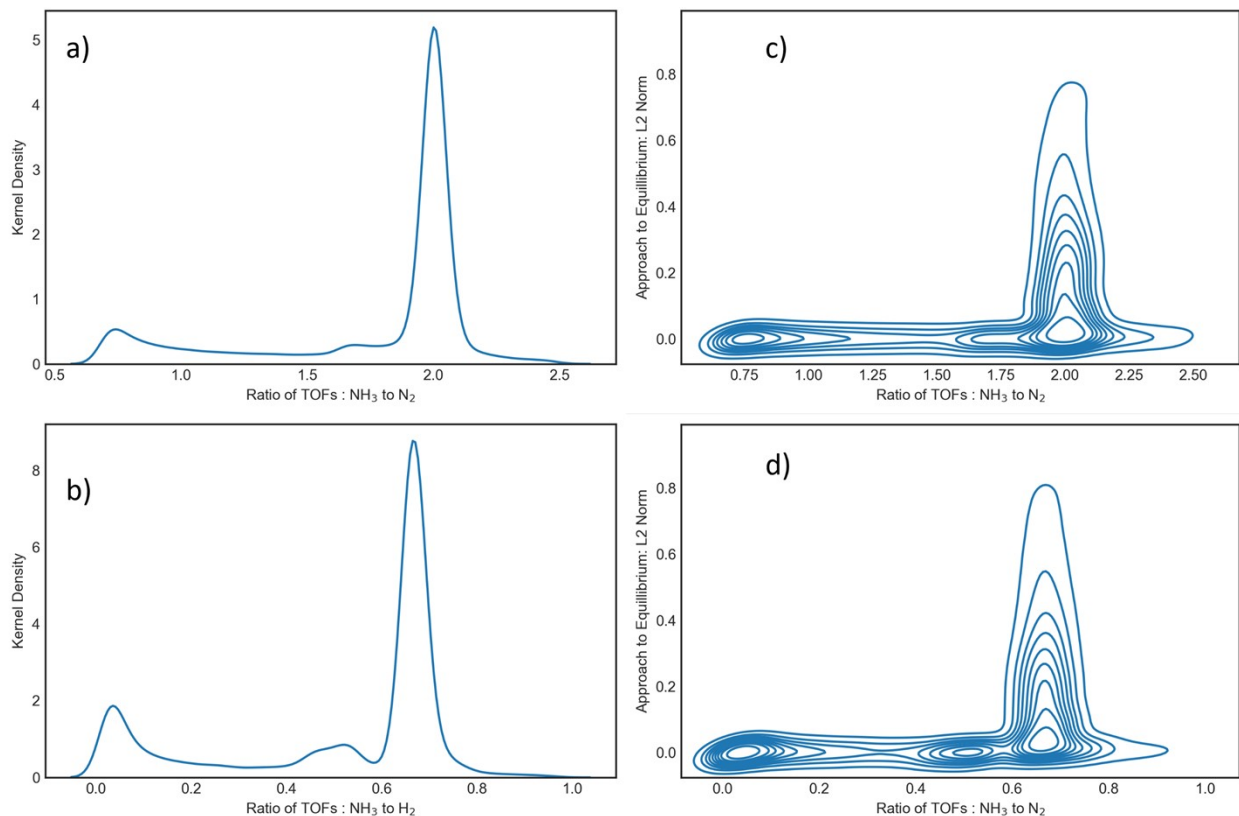


Figure S6. Kernel Density plot for the ratio of species turnovers (TOFs) predicted by DNN. a) NH_3 to N_2 (ideally should be 2.0). b) NH_3 to H_2 (ideally should be $2/3$). Kernel density contours for the ratio of TOFs (x-axis) and the

distance from equilibrium (y-axis) at the composition, temperature, and pressure at which TOFs were evaluated for c) NH_3 to N_2 and d) for NH_3 to H_2 .

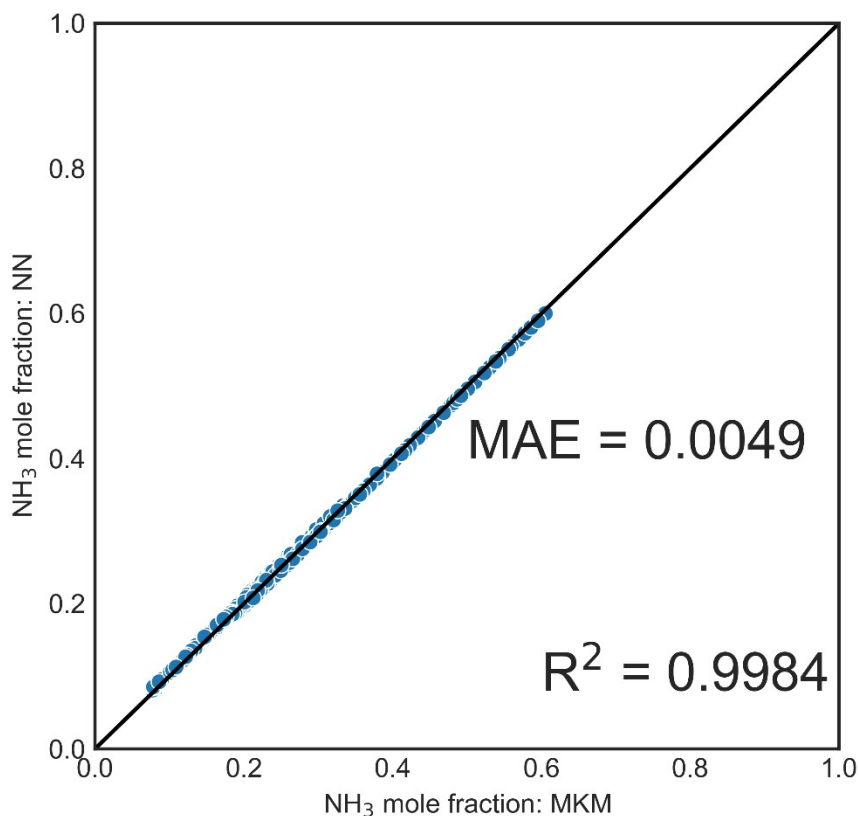


Figure S7. Parity plot for NH_3 mole-fraction from 1,200 PFR simulations using a DNN-surrogate Python-ODE solver model (y-axis) vs. the MKM (x-axis) simulation. TOFs of all species are trained and predicted by the surrogate model.

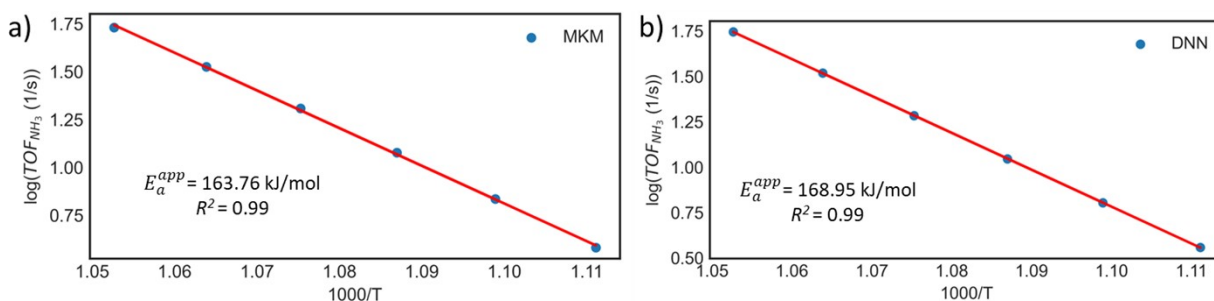


Figure S8 Apparent Activation Energy Estimation from Arrhenius Plots depicting log-normalized Turnover Frequencies (TOFs) of NH_3 (y-axis) against $1000/T$ (x-axis, T in Kelvin) for NH_3 reduction chemistry. Predictions are provided for: a) full-order MKM, and b) DNN-surrogate-based model. The TOFs are derived from the first CSTR reactor (PFR is represented as a series of CSTRs). NH_3 -TOFs are measured in (1/s), while temperature (T) is measured in Kelvin. The total reactor pressure is 1 atm, and the volumetric flow rate is $0.1 \text{ cm}^3/\text{s}$.

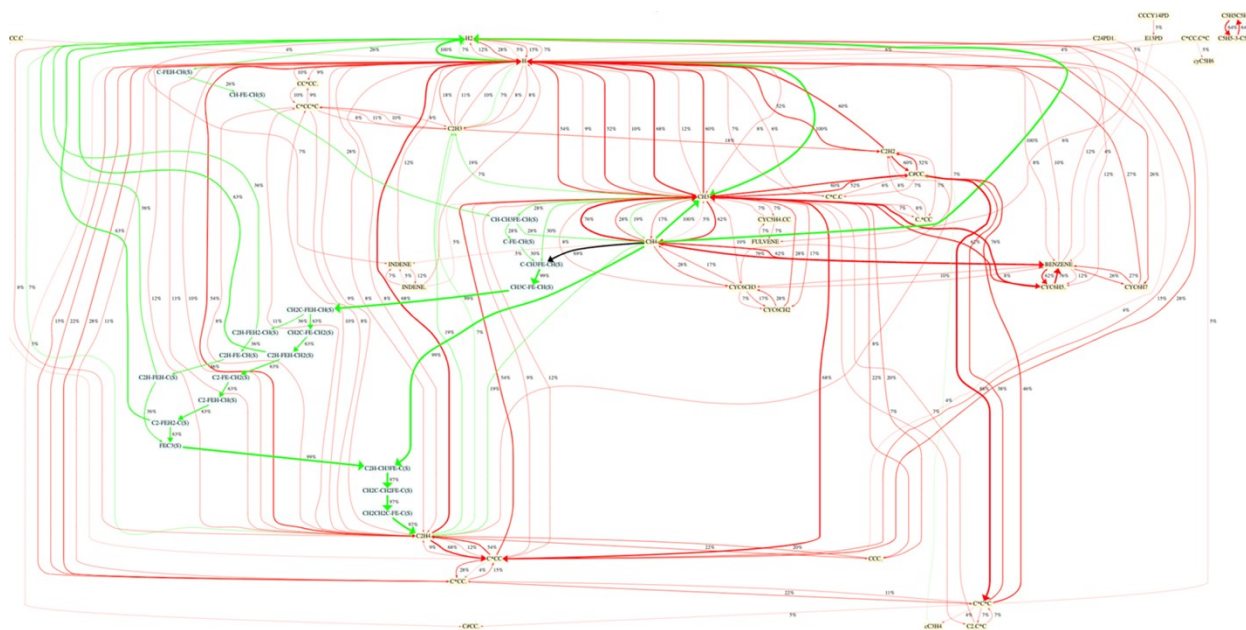


Figure S9. Reaction Path Analysis (RPA) for the methane MKM¹ with 540 species and 9,333 reactions.

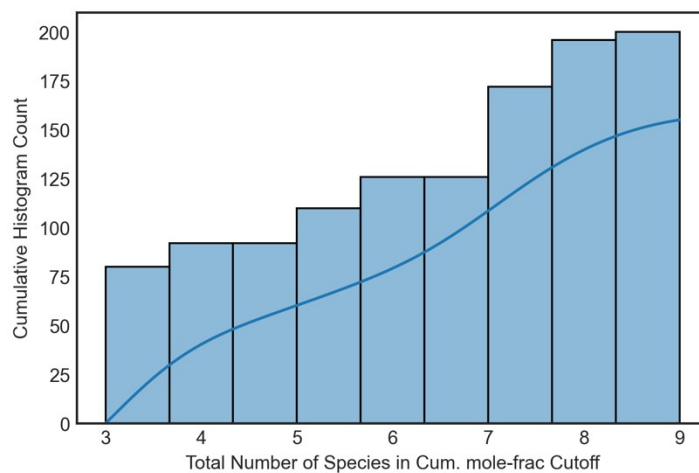


Figure S10. Cumulative histogram plot of the minimum number of key species present in the outlet of 200 PFR reactor simulations that make up 99.5 mole percent. Here, for ~75 simulations in the dataset, only 3 species describe the 99.5 mole percent at the exit and so forth up to a total of 9 species for the entire dataset. The list of these key species and the percentage of their occurrence (within the training dataset) is outlined in Table S1.

Table S1. List of key long-lived species (cumulating to 99.5 mole-percent) present at the reactor exit in 200 PFR reactor simulations. The percentage of occurrence in these simulations is also shown in the last column. Here, for instance, C₂H₄ appears in the cumulative cutoff only 60% of the training dataset (120 times out of the 200 simulations).

No.	Species Name	Present at PFR outlet (in %)
1	CH ₄	100.0

2	H ₂	100.0
3	N ₂	100.0
4	C ₂ H ₄	60.0
5	C ₂ H ₂	54.0
6	C ₃ H ₆	37.5
7	C ₃ H ₄	14.50
8	C ₆ H ₆	36.5
9	C ₇ H ₈	9.50

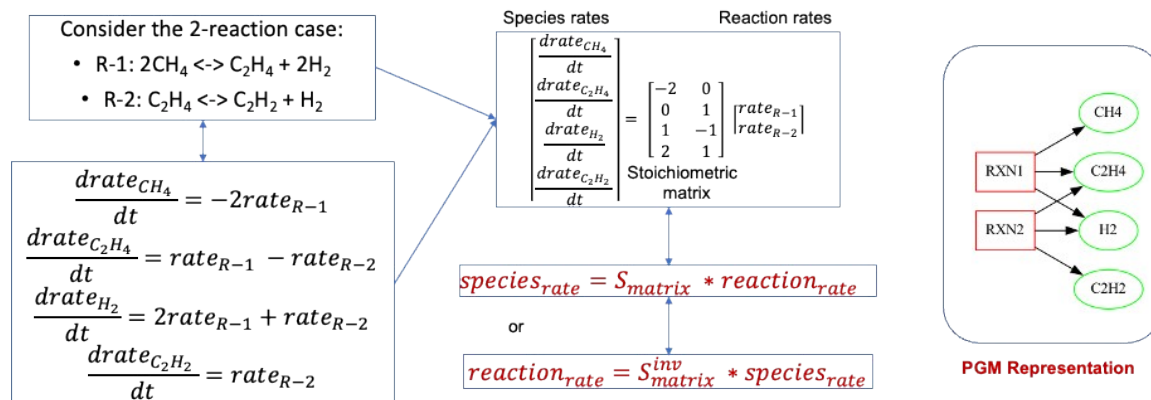
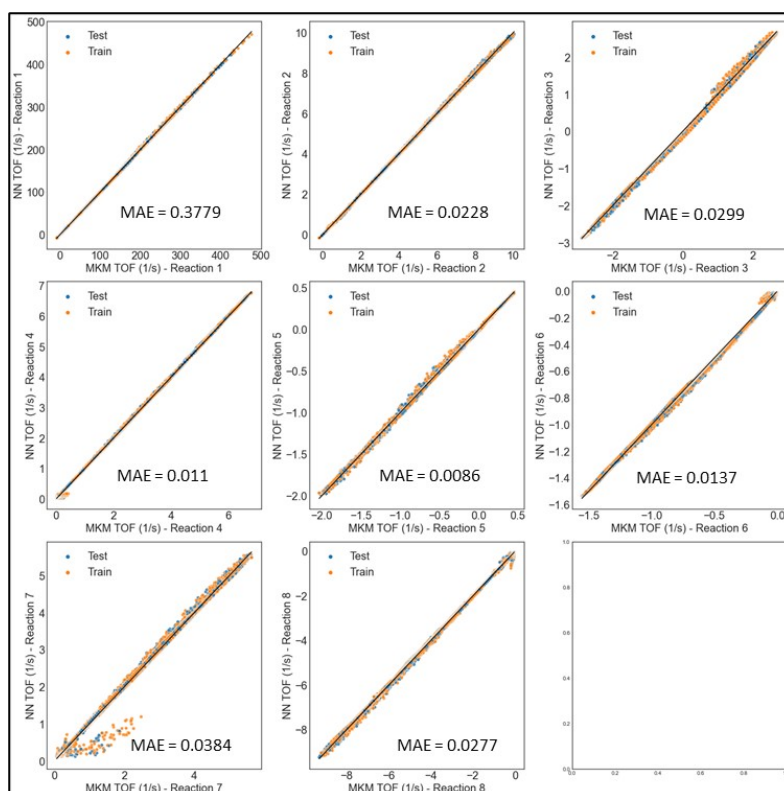


Figure S11. Schematic of two overall reactions connecting CH₄, C₂H₄, C₂H₂, H₂, as linear system of equations (Y = SX), involving the stoichiometry matrix and a probabilistic graph model (PGM) representation.

a)



b)

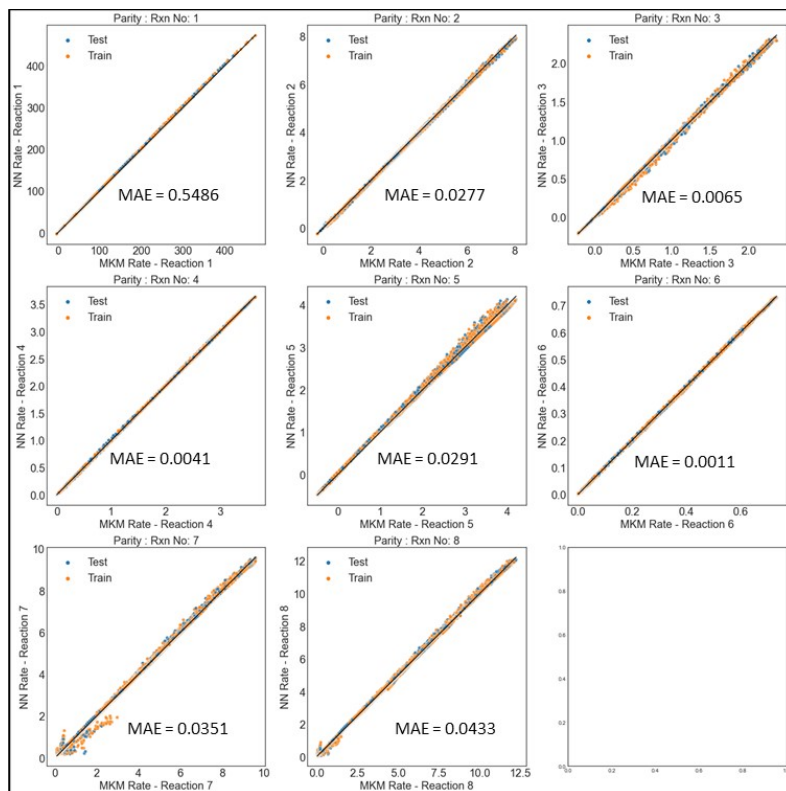


Figure S12. Parity plots between DNN based point prediction of overall reaction turnovers (TOFs) (y-axis) vs. calculated overall reaction TOFs from MKM simulation data (x-axis) for a) an arbitrary set of reactions (set A), and b) a mathematically convenient set of reactions (set B). Each subplot represents a given overall reaction with the order of reaction numbers going from left to right 1, 2, 3 (first row); and going top to bottom 1, 4, 7 (first column).

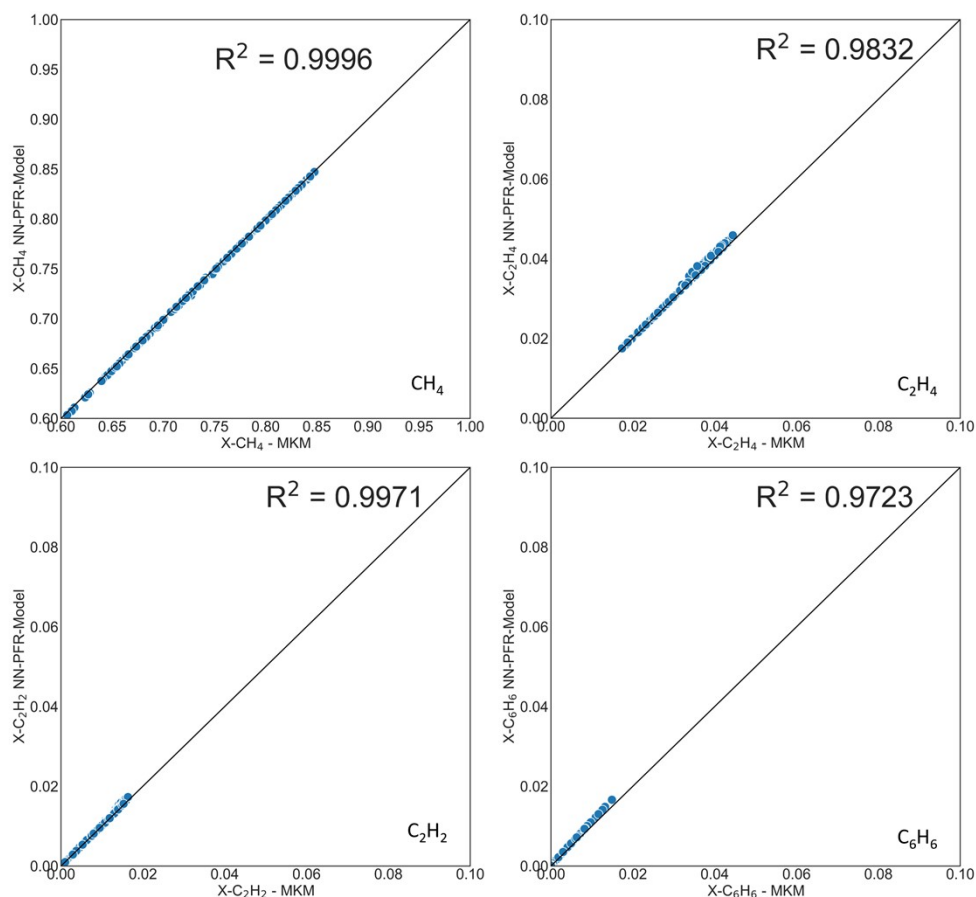


Figure S13. Parity plots for PFR-exit mole fractions of major species: CH₄, C₂H₄, C₂H₂, C₆H₆ from the DNN-based surrogate model of PFR simulation (y-axis) vs. and MKM simulation (x-axis), for an arbitrary set of reactions (set A) when the trace reactions (reaction no: 7 and 8) are ignored.

Table S2. Overall reaction rates and DNN training error statistics by uncertainty quantification (UQ) for the reaction set A. Trace reactions (7 and 8) are not considered.

Reaction No.	Reaction TOF (1/s)			Global Error Metrics	
	Maximum	Minimum	Mean	Mean	Std. Dev.
1	478.83	-2.84	51.06	-0.017723	0.829502
2	9.26	-0.19	4.35	-0.000874	0.052006
3	2.90	-0.35	0.86	0.000039	0.021066
4	5.26	-0.50	0.85	-0.000362	0.017502
5	0.37	-4.51	-1.61	0.001076	0.034952
6	0.12	-1.15	-0.25	0.000018	0.005914

Table S3. Overall reaction rates and DNN training error statistics by uncertainty quantification (UQ) for the reaction set B. Trace reactions are considered.

Reaction No.	Reaction TOF (1/s)			Global Error Metrics	
	Maximum	Minimum	Mean	Mean	Std. Dev.
1	473.53	-2.75E+00	44.73	0.06779	0.035663

2	8.06	-2.37E-01	2.73	-0.00044	0.015203
3	2.37	-2.18E-01	0.46	-0.00132	0.012483
4	3.65	1.45E-11	0.59	-0.00015	0.033927
5	4.21	-4.81E-01	1.47	-0.00025	0.002828
6	0.73	1.68E-14	0.11	0.000063	0.085209
7	9.60	8.12E-02	3.45	-0.00785	0.069956
8	12.23	5.26E-02	4.35	-0.00057	0.035663

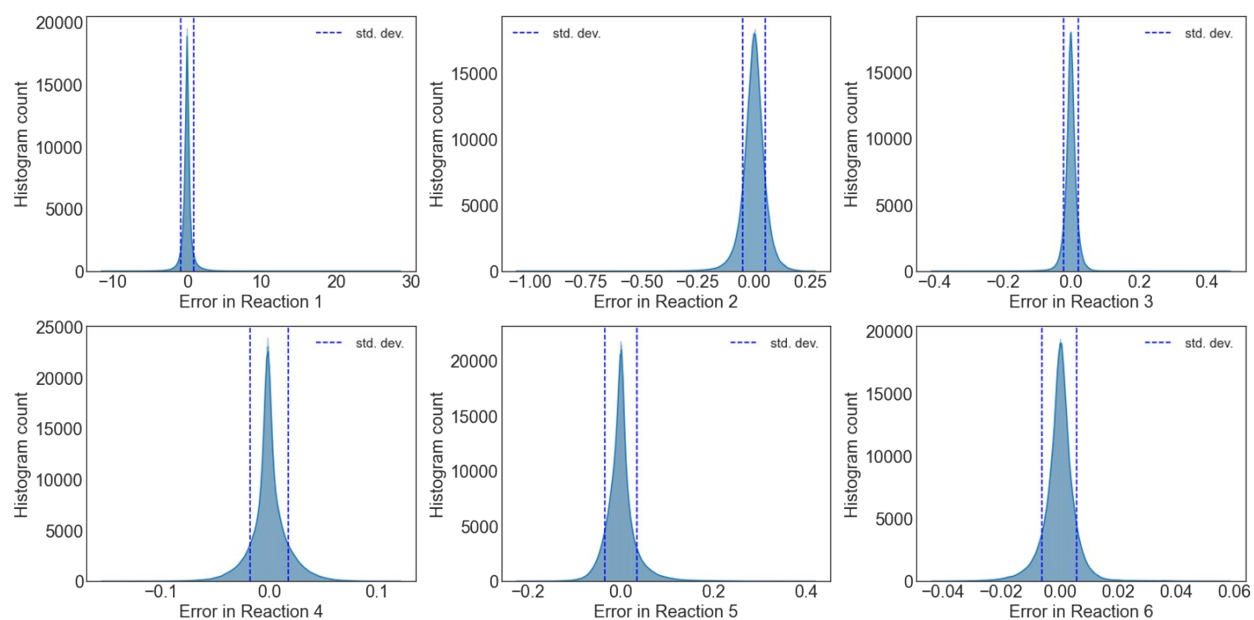


Figure S14. Uncertainty Quantification of Neural Network Training error for a cumulative of 100 independent neural networks trained on the reaction set A (trace reactions are not considered). Errors are deviations of overall rates between NN predictions and MKM calculations. Errors in rates are in units (1/s).

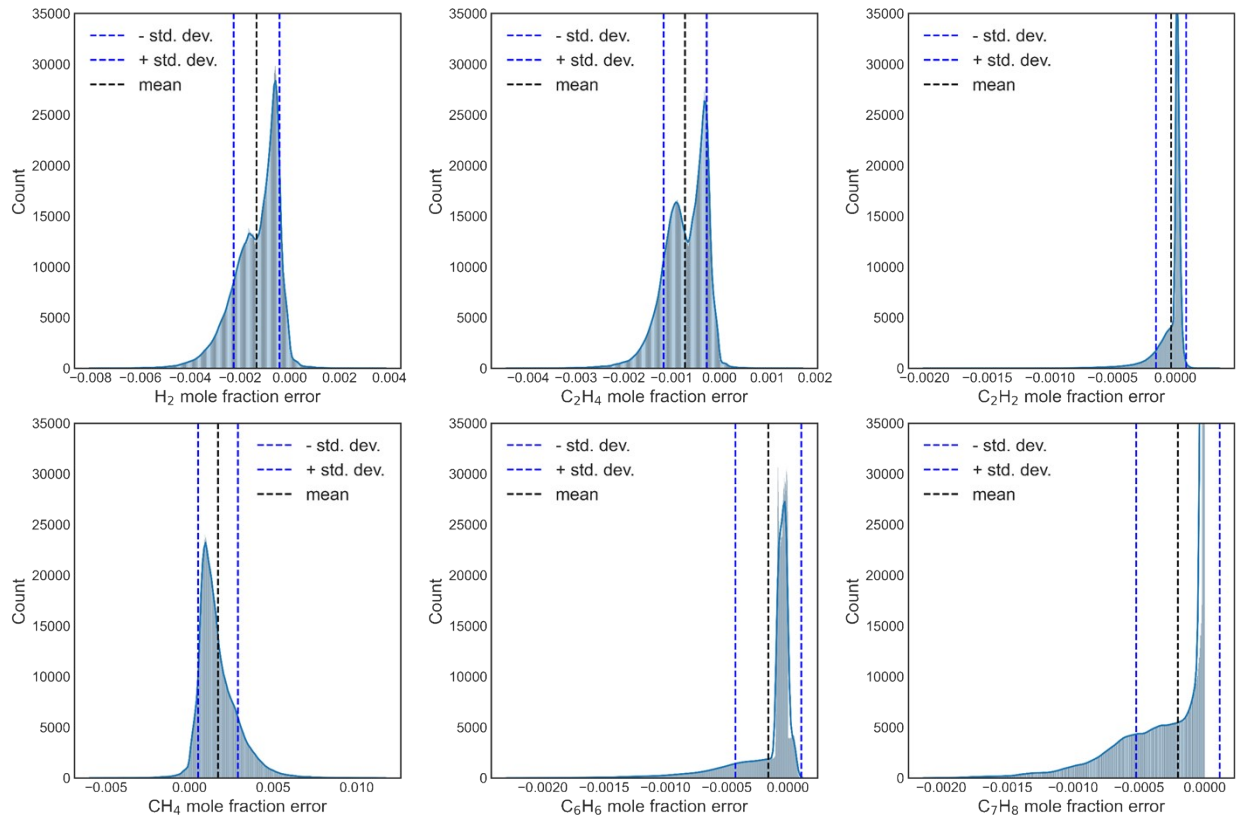


Figure S15. DNN-based PFR integration propagation error for exit mole-fractions of major species considered for the reaction set A (trace reactions are not considered). x-axis represents mole fractions.

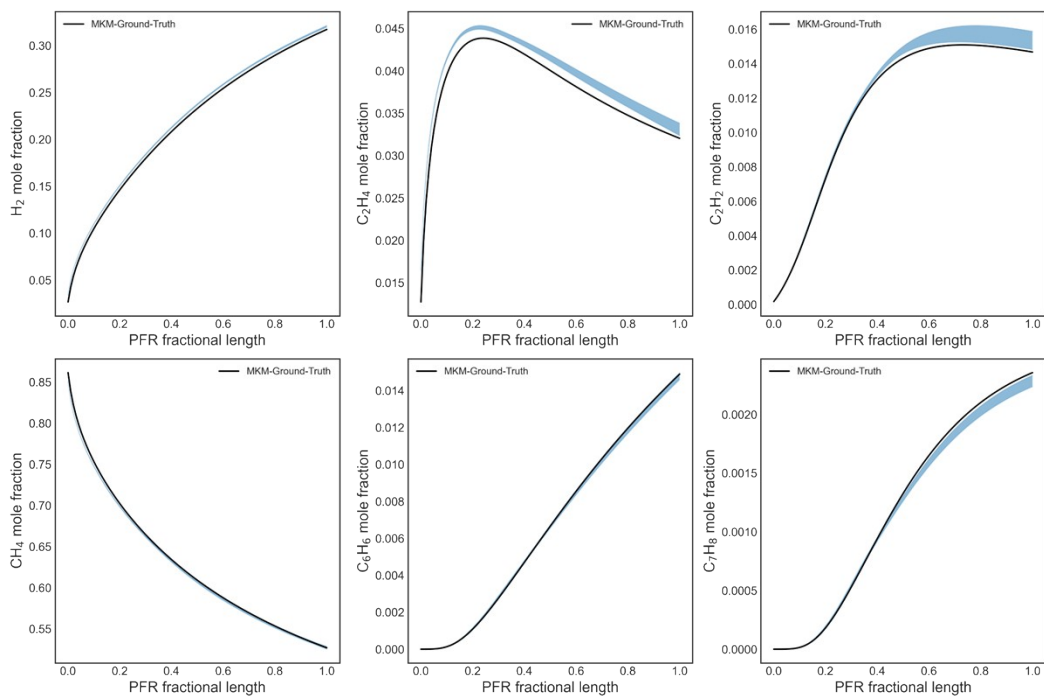


Figure S16. PFR integration spatial profiles for mole fractions of major species in the reaction set A (trace reactions are not considered). Temperature is 1290.75 K and volumetric flow rate is $0.026 \text{ cm}^3\text{s}^{-1}$. Black line represents the

ground truth from the full-order MKM. Thick blue represents the bounds (mean \pm standard deviation) of the DNN-based PFR predictions for 100 independent neural networks.

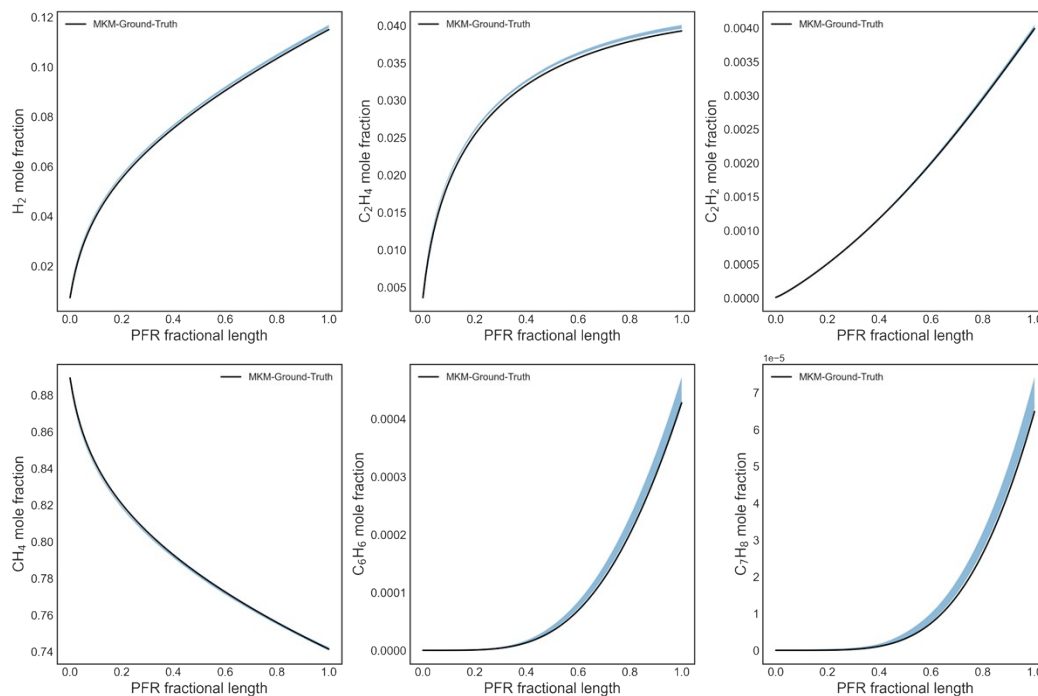


Figure S17. PFR spatial profiles for mole fractions of major species in reaction set A (trace reactions are not considered). Temperature is 1259.25 K and volumetric flow rate is 0.098 cm³s⁻¹. Black line represents the ground truth from the full-order MKM. Thick blue represents the bounds (mean \pm standard deviation) of the DNN-based PFR predictions for 100 independent neural networks.

References

1. Toraman, H. E.; Alexopoulos, K.; Oh, S. C.; Cheng, S.; Liu, D.; Vlachos, D. G., Ethylene production by direct conversion of methane over isolated single active centers. *Chemical Engineering Journal* **2021**, *420*, 130493.